HHS Public Access

Author manuscript

Vision Res. Author manuscript; available in PMC 2024 February 01.

Published in final edited form as:

Vision Res. ; 203: 108157. doi:10.1016/j.visres.2022.108157.

Photoreceptor Function and Structure in Retinal Degenerations caused by Biallelic *BEST1* Mutations

Artur V. Cideciyan[a,1], **Samuel G. Jacobson**[a], **Alexander Sumaroka**[a], **Malgorata Swider**[a], **Arun K. Krishnan**[a], **Rebecca Sheplock**[a], **Alexandra V. Garafalo**[a], **Karina E. Guziewicz**[b], **Gustavo D. Aguirre**[b], **William A. Beltran**[b], **Yoshitsugu Matsui**[c], **Mineo Kondo**[c], **Elise Heon**[d]

[a]Scheie Eye Institute, Department of Ophthalmology, Perelman School of Medicine, University of Pennsylvania, Philadelphia, PA 19104, USA

[b]Division of Experimental Retinal Therapies, Department of Clinical Sciences and Advanced Medicine, School of Veterinary Medicine, University of Pennsylvania, Philadelphia, PA 19104, USA

[c]Department of Ophthalmology, Mie University Graduate School of Medicine, Tsu, Japan

[d]Department of Ophthalmology and Vision Sciences, The Hospital for Sick Children, University of Toronto, Toronto, ON M5G 2L3, Canada

Abstract

The only approved retinal gene therapy is for biallelic *RPE65* mutations which cause a recessive retinopathy with a primary molecular defect located at the retinal pigment epithelium (RPE). For a distinct recessive RPE disease caused by biallelic *BEST1* mutations, a pre-clinical proof-of-concept for gene therapy has been demonstrated in canine eyes. The current study was undertaken to consider potential outcome measures for a *BEST1* clinical trial in patients demonstrating a classic autosomal recessive bestrophinopathy (ARB) phenotype. Spatial distribution of retinal structure showed a wide expanse of abnormalities including large intraretinal cysts, shallow serous retinal detachments, abnormalities of inner and outer segments, and an unusual prominence of

[1]Correspondence at cideciya@pennmedicine.upenn.edu.

Artur V. Cideciyan: Conceptualization, Formal analysis, Investigation, Writing - Original Draft, Writing - Review & Editing, Supervision
Samuel G. Jacobson: Conceptualization, Investigation, Writing - Original Draft, Writing - Review & Editing, Supervision
Alexander Sumaroka: Investigation, Formal analysis
Malgorata Swider: Formal analysis
Arun K. Krishnan: Investigation
Rebecca Sheplock: Investigation, Project administration
Alexandra V. Garafalo: Investigation, Project administration
Karina E. Guziewicz: Writing - Review & Editing
Gustavo D. Aguirre: Writing - Review & Editing
William A. Beltran: Writing - Review & Editing
Yoshitsugu Matsui: Resources
Mineo Kondo: Resources, Writing - Review & Editing
Elise Heon: Resources, Writing - Review & Editing

Disclosure: AVC, SGJ, KEG, GDA, and WAB are listed as co-inventors on US Patent Applications related to treating bestrophinopathies.

the external limiting membrane. Surrounding the central macula extending from 7 to 30 deg eccentricity, outer nuclear layer was thicker than expected from a cone only retina and implied survival of many rod photoreceptors. Co-localized however, were large losses of rod sensitivity despite preserved cone sensitivities. The dissociation of rod function from rod structure observed, supports a large treatment potential in the paramacular region for biallelic bestrophinopathies.

Retinal diseases caused by *BEST1* mutations (bestrophinopathies) are a member of a group of complex monogenic conditions that are inherited both in autosomal dominant and autosomal recessive forms (Johnson et al., 2017). Other retinopathies in this growing group include those caused by mutations in *IMPG1* and *IMPG2* which can result in phenotypes overlapping with bestrophinopathies (Brandl et al., 2017), as well as those with distinctly different phenotypes caused by monoallelic and biallelic mutations in *RHO* (Azam et al., 2009; Dryja et al., 1990, 1993; Rosenfeld et al., 1992;), *CRX* (Freund et al., 1997; Jacobson et al., 1998), *GUCY2D* (Sharon et al., 2018), *RPE65* (Bowne et al., 2011; Hull et al., 2016; Marlhens et al., 1997), *RP1* (Guillonneau et al 1999; Huckfeldt et al., 2020), *PROM1* (Cehajic-Kapetanovic et al., 2019; Maw et al., 2000*), SNRNP200* (Gerth-Kahlert et al., 2019), *PRPH2* (Daftarian et al., 2019; Farrar et al., 1991; Kajiwara et al., 1991; Wang et al., 2013), *GNAT1* (Dryja et al., 1996; Naeem et al., 2012), *SAG* (Fuchs et al., 1995; Sullivan et al., 2017), and *RDH12* (Perrault et al., 2004; Sarkar et al., 2020). Monoallelic mutations in *BEST1* can be non-disease-causing, or cause autosomal dominant Best vitelliform macular dystrophy (BVMD) or autosomal dominant adult-onset vitelliform macular dystrophy (Krämer et al., 2000; Marquardt et al., 1998; Petrukhin et al., 1998; Seddon et al., 2001). More rarely autosomal dominant forms of vitreoretinochoroidopathy, microcornea, rod-cone dystrophy, cataract, and posterior staphyloma have been also associated with monoallelic mutations in *BEST1* (Chen et al., 2016; Yardley et al., 2004). Biallelic mutations in *BEST1* cause the distinct autosomal recessive bestrophinopathy (ARB) phenotype (Burgess et al., 2008; Schatz et al., 2006).

The classic examples of juvenile-onset monoallelic *BEST1* disease show pathognomonic macular lesions centered on or near the fovea and the disease is thought to progress through stages descriptively named based on their ophthalmoscopic appearances such as vitelliform, pseudohypopyon, or vitelliruptive (Boon et al., 2009; Johnson et al., 2017; Marmorstein et al., 2009). However retinal disease in so-called vitelliform macular dystrophy (VMD) phenotype is not always limited to the central macula considering reports of one or more satellite lesions forming in what has been named multifocal vitelliform dystrophy (Boon et al., 2007; Maruko et al., 2006; Miller, 1977; Sodi et al., 2007). Satellite lesions tend to be located approximately at the eccentricity of the optic nerve possibly corresponding to the ‘rod ring’ – an annular region of high rod density in human retinas (Curcio et al., 1990).

Initial recognition of the biallelic *BEST1* disease was associated with a retinopathy that appeared substantially different from the classic lesions observed in the monoallelic forms (Burgess et al., 2008; Schatz et al., 2006). Despite the retina-wide RPE involvement evidenced by EOG changes in both mono- and bi-allelic forms, only the latter was thought to involve photoreceptor dystrophy as evidenced by abnormal ERGs (Burgess et al., 2008). Consistently, biallelic *BEST1* disease was thought to involve a large retinal area that

included the macula as well as the perimacular and midperipheral regions, as opposed to the foveal vitelliform lesions in VMD. Within the involved areas, there were extensive cystic changes in the retina variably described as “macular edema”, “cystic edema”, “intraretinal cysts”, “cystoid intra-retina fluid”, “retinoschisis”, or “cystoid maculopathy” (Boon et al., 2013; Burgess et al., 2008; Fung et al., 2015; Kinnick et al., 2011; Schatz et al., 2006; Silva et al., 2013). Cystic spaces were often located within the inner nuclear layer and sometimes in the ganglion cell layer and the outer nuclear layer. Often a shallow subretinal serous detachment was found to extend across the macula. Later stages of disease with greater photoreceptor degeneration seemed to have less cystic changes as if functioning photoreceptors were required for the accumulation of intraretinal fluid.

Over the years it has become clear that not all bilallelic *BEST1* disease results in ARB phenotype – some patients show a VMD phenotype normally associated with monoallelic disease (Bitner et al., 2011; Khan et al., 2018; Kinnick et al., 2011; Sodi et al., 2011). The exact genotype-phenotype relationship remains elusive, but it has been hypothesized that complete inactivation of the gene on both alleles results in the ARB phenotype, whereas an allele with a dominant negative effect results in the VMD phenotype (Pomares et al., 2012).

Detailed visual function consequences co-localized with detailed photoreceptor structure abnormalities are not well understood in patients with biallelic *BEST1* mutations. To plan for upcoming gene therapy trials (Guziewicz et al., 2018), we evaluated rod- and cone-photoreceptor mediated function in patients exhibiting the more commonly encountered ARB phenotype.

Methods

Subjects

There were four ARB patients (ages 22–39; Table 1) from three families. Patients were compound heterozygous for *BEST1* gene mutations (Table 1). Some results from two of the patients (P1 and P2) were previously published (Guziewicz et al., 2018), and some of those results are duplicated in the Supplement for ease of comparability. Next generation sequencing through CLIA (Clinical Laboratory Improvement Amendments) approved laboratories was used to identify variants in P1, P2 and P3, and whole exome sequencing was used to identify variants in P4. The pathogenicity of variants identified was interpreted according to the American College of Medical Geneticists guidelines (Richards et al., 2015). Procedures followed the Declaration of Helsinki, and the study was approved by the Institutional Review Board (IRB) of the University of Pennsylvania. Informed consent, assent, and parental permission were obtained, and the work was HIPAA-compliant.

Measures of rod and cone function

Dark-adapted chromatic perimetry (DACP) was used to measure rod-mediated function across the visual field (Cideciyan et al., 2021; Jacobson et al., 1986). Mediation of the 500 nm (blue-green) stimulus (1.7° diameter; 200 ms duration) sensitivity by rod photoreceptors was determined by comparison of sensitivities with a 650 nm (red) stimulus and taking advantage of the spectral sensitivity differences between rods and cones. Light-adapted

chromatic perimetry (LACP) with a 600 nm (orange) stimulus was used to measure cone-mediated function (Cideciyan et al., 2021; Jacobson et al., 1986).

Dark-adaptation kinetics was evaluated similar to techniques previously described (Cideciyan et al., 1997, 2000; Guziewicz et al., 2018) using a LED based dark-adaptometer (Roland Consult, Brandenburg a.d. Havel, Germany) and taking advantage of a short duration (30 s) moderate light exposure performed during standard of care from a short-wavelength autofluorescence imaging device (25% laser output; Spectralis HRA; Heidelberg Engineering, Heidelberg, Germany).

Retinal imaging

A confocal scanning laser ophthalmoscope (Spectralis HRA, Heidelberg Engineering, Heidelberg, Germany) was used in three patients (P1, P2, and P3) to obtain short-wavelength excited reduced-illuminance autofluorescence imaging (SW-RAFI) (Cideciyan et al., 2007). Wide field image montage was assembled by manually specifying corresponding retinal landmark pairs in overlapping segments using custom-written software (MATLAB 6.5). In one patient (P4), ultra-widefield autofluorescence imaging (Optos, Marlborough, MA, USA) was used.

Optical coherence tomography (OCT) was performed with a spectral-domain (SD) OCT system (RTVue-100, Optovue Inc., Fremont, CA) in three patients (P1, P2, and P3), and a clinical ultrahigh resolution (UHR) SDOCT system (Bi-μ; Kowa Company, Ltd., Tokyo, Japan) was used in two patients (P3 and P4) to better understand microscopic features. In three of the patients (P1, P2, and P3), serial OCT studies performed in the referring clinic were available. Our recording and analysis techniques have been published (Cideciyan & Jacobson, 2019; Cideciyan et al., 2013, 2020; Jacobson et al. 2016).

Results

Molecular and clinical findings

P1 carried two missense mutations in *BEST1* within the cytoplasmic domain of the protein (Table 1); both parents were heterozygote carriers and reported to be unaffected. The c.341T>C variant is highly conserved, is not reported in publicly available databases. The pathogenicity scores predict this variant to be pathogenic. The c.400C>G variant involves a highly conserved amino acid, is very rare and predicted to be likely pathogenic. Variants seen siblings P2 and P3 affect the first transmembrane domain of the protein (Table 1). Parents were heterozygote carriers and reported to be unaffected. The c.95T>C variant is highly conserved, not seen in any of the public control databases and is predicted to be likely pathogenic (Jespersgaard et al., 2019). While the synonymous variant at codon 34 that has been previously predicted to alter splicing, causing a frameshift and a downstream truncation and considered pathogenic (Davidson et al., 2010). P4 carried a missense mutation commonly identified in Asian *BEST1* patients (Kubota et al., 2016; Luo et al., 2019; Nakanishi et al., 2016; Tian et al., 2017) and another variant predicted to be pathogenic (Nakanishi et al., 2016).

Best corrected ETDRS visual acuities in the eight eyes ranged from −0.18 to 0.72 logMAR (Table 1) and were within the range published in other patients with biallelic *BEST1* mutations and ARB or VMD phenotype (Suppl. Fig.S1). Fixation in the right eyes of P1-P3 was at or near the fovea and relatively stable (bivariate contour ellipse areas ranging from 0.6 to 1.9 deg^2); fixation of left eyes of P1-P3 was not formally evaluated. The retained acuities of P4 (Table 1) implied foveal fixation but this was not formally evaluated. P1 had a history of angle closure glaucoma and cataract surgery in both eyes; P2 and P3 were phakic in both eyes (Table 1). P4 had a history of angle-closure glaucoma and had undergone laser iridotomy in the left eye. Axial lengths were not measured.

Prominence of external limiting membrane and other retinal features

Qualitatively, all eyes showed substantial abnormalities of retinal cross-sectional structure that extended from foveal to mid-peripheral regions (Fig.1). Abnormalities included large intraretinal cysts located mostly in the INL (Fig.1, arrows ‘a’) but also sometimes in the ONL (Fig.1, arrows ‘b’), shallow serous retinal detachments (Fig.1, arrows ‘c’), and abnormalities of structures extending from the ELM to the RPE. There was an unusual prominence of the ELM peak (Fig.1, arrows ‘d’ in panels A and B) which has been previously described in some disease stages of a different genetic form of macular degeneration (Lee et al., 2014) but not to our knowledge in mono- or bi-allelic forms of *BEST1* disease. In some locations there was local enhancement of IS/OS intensity (Fig.1, arrows ‘e’). Extending into the serous subretinal detachments were stalactite-like reflective material (Fig.1, arrows ‘f’) that have been hypothesized (Marmorstein et al., 2018) to represent outer segments elongated due to impaired phagocytosis. It is also possible that these structures originated from glial cells considering the distinct prominence of the ELM.

Photoreceptor structure

ONL thickness in patients was abnormally reduced but detectable across the central approximately 60-degree diameter region (Fig.2A). In 4 of 6 eyes where such measures were available there was relative preservation of the parapapillary area as described previously in ARB (Birtel et al., 2020), as well as in *ABCA4*-STGD (Cideciyan et al., 2005) and *RDH12*-LCA (Aleman et al., 2018). At 35–40 degree eccentric in the nasal retina and at 25–30 degree eccentric in the temporal retina, there were distinct transitions associated with increases in the ONL thickness with greater eccentricity which often reached normal limits more peripherally (Fig.2A). Retinal laminae distal to the ONL were evaluated in detail at a locus near 25 degrees in the nasal retina where ONL was substantially thinned in six eyes (Fig.2B, Retinal Location I), as well as at a locus near 45 degrees in the nasal retina where ONL could be comparable to normal or only mildly thinned (Fig.2C, Retinal Location II).

At 25 degrees eccentric in the nasal retina, best retained lamination was in P1-OS and P3-OD (Fig.2B). There were distinct ELM and IS/OS peaks with a presumed IS length that approximated normal. ELM peak was unusually prominent. COST and ROST peaks could not be individually distinguished; distance from IS/OS to RPE was comparable to normal. P3-OS and P1-OD showed some lamination distal to the ELM but the identities of the peaks could not be confirmed. P2-OS and P2-OD showed an unusually prominent ELM peak the

identity of which was confirmed by following the peak laterally to neighboring regions with greater preservation; there was no lamination apparent between ELM and RPE (Fig.2B).

At 45 degrees eccentric in the nasal retina, best retained lamination was in P1-OS with outer retinal laminae comparable to normal despite a thinned ONL and a challenging ROST peak localization (Fig.2C). Intensity of the ELM was enhanced, and the intensities of the IS/OS and COST bands were reduced compared to normal. Length of IS and COS appeared to be comparable to normal. P3-OD, P3-OS and P2-OS showed mostly interpretable lamination. ELM signal intensity appeared to be higher than normal and IS/OS signal lower than normal, with an IS length that was comparable to normal in P3-OD and P3-OS. For P1-OD and P2-OD there was greater noise and laminations were more tenuous but consistent with the other eyes. In all eyes ROST peak was difficult to distinguish but distance from IS/OS to RPE was comparable to normal except in P2-OD which showed mild reduction. It is important to note that in many cases there was an apparent hypo-scattering layer between COST and RPE peaks and a microdetachment of the retina from the RPE similar to that seen in dogs with biallelic *BEST1* mutations (Guziewicz et al., 2018) cannot be specifically ruled out.

SW-RAFI showed abnormalities consisting of spatial heterogeneity of signal extending to the midperiphery which was well correlated with the OCT abnormalities in six eyes (Suppl. Figs. S2–S7). In the nasal periphery of each eye, there was a distinct transition to local homogeneity in SW-RAFI signal corresponding to greater thickness of ONL and less outer retinal laminar abnormalities observed on OCT (Suppl. Figs. S2–S7). More limited data from both eyes of P4 (Suppl. Fig. S8) were comparable.

Longitudinal changes in retinal structure

Additional imaging studies were performed in P1, P2 and P3 at different ages (Suppl. Fig. S9). Main changes detectable with the available data involved the fluctuation of intraretinal cysts. Specifically, there were examples where cysts visible within the ONL became undetectable at other visits or vice versa. There were also examples of INL cysts substantially changing in size and extent. In addition, subretinal fluid extent and localization could be seen to change. Some of the smaller fluctuations could be due to inexact matching of the scan locations at different visits, but some of the larger fluctuations could not be explained with scan location and must reflect physiological changes occurring in the retina. Evaluation of potential longitudinal changes in the outer retina relevant to progressive photoreceptor degeneration (such as ONL thickness or OS length) was not possible with the data available.

Retinal function – evidence for treatment potential

Rod and cone sensitivities were sampled densely (every 2 deg) along the horizontal and vertical meridians in the central and mid-peripheral retina, and sparsely (12 deg grid) across the full visual field, and co-registered to retinal structure (Suppl. Figs. S2–S7). In general, there were large losses of rod sensitivity across the swath of central and midperipheral retina that unsurprisingly showed OCT and SW-RAFI abnormalities. Beyond 30–50 degrees eccentric from the fovea, where retinal structure normalized, rod function

also approached normal in the superior, inferior and temporal visual fields (Suppl. Figs. S2–S7 E). The furthest tested eccentricity (48 deg) in the nasal visual field remained abnormal in all evaluated eyes. In four of the eyes (P1-OD, P1-OS, P3-OD, P3-OS), there was evidence of parapapillary region of relatively better rod function consistent with the parapapillary retention of retinal structure (Suppl. Figs. S2–S7). Cone sensitivities were generally substantially better preserved as compared to rod sensitivities. At many loci within the central and mid-peripheral areas of clear-cut retinal structural defects, cone sensitivities were within or near normal limits, or showed mild losses of less than 1 log unit. Of interest, near normal cone sensitivities could include retinal regions with serous detachments (e.g. P3-OD, temporal to fovea) and large intraretinal cystic spaces (e.g. P2-OS, nasal to the fovea).

To determine whether large losses of rod sensitivity with retained cone sensitivity were due to severe degeneration of rod cells whilst cone cells survived, we evaluated co-localized measures of ONL thickness and sensitivity (Fig.3). By imaging methods available to date, rod and cone nuclei within the ONL are not directly distinguishable by their backscatter characteristics. However, we have previously estimated the fraction of the ONL containing cone nuclei as a function of eccentricity in normal eyes (Cideciyan et al., 2020). Near the fovea, ONL thickness remaining in ARB eyes was well within the possibility of a cone-only retina and thus evidence for remnant but dysfunctional rod cells was not obtainable. Existence of a rod or cone treatment potential within the central ~14 deg diameter region of the macula is currently indeterminate. Beyond ~30–40 deg in the nasal retina both structure and function approached normal and thus there is no large treatment potential in terms of short-term improvement of visual function. Between ~7 and ~30 deg eccentricity nasal to the fovea, retained ONL thickness in ARB was well beyond that expected from a pure cone retina. Similarly, beyond ~7 deg eccentric in the temporal retina, there was ONL thickness likely including substantial rod nuclei. Both regions had rod function disproportionately reduced and strongly suggest remaining rod photoreceptors lacking function with a large magnitude treatment potential in terms of a short-term improvement of visual function.

Retinal function – kinetics of rod dark-adaptation

All photoreceptor cells require a photolabile opsin molecule to signal light and the universal chromophore for all opsin molecules is 11-cis-retinal. There are now at least three known cycles that constantly regenerate 11-cis-retinal for continual vision (Palczewski & Kiser, 2020). For rod photoreceptors, the bulk of the 11-cis-retinal originates from RPE cells within the so-called canonical visual cycle. We recorded dark-adaptation kinetics of the rod system to estimate the speed of the canonical visual cycle (Lamb & Pugh, 2004). All three patients studied demonstrated abnormally slow kinetics of dark-adaptation recovery (Suppl. Fig. S10).

Discussion

Genotype-phenotype in biallelic *BEST1* mutations – review of literature

Following the initial two reports (Burgess et al., 2008; Schatz et al., 2006), there has been a growing list of publications describing autosomal recessive retinal disease caused by

biallelic *BEST1* mutations (Birtel et al., 2020; Bitner et al., 2011; Boon et al., 2013; Chen et al., 2016; Davidson et al., 2010; Dev Borman et al., 2011; Fung et al., 2015; Habibi et al., 2019; Iannaccone et al., 2011; Jansson et al., 2016; Khan et al., 2018; Kinnick et al., 2011; Kubota et al., 2016; Lee et al., 2015; Luo et al., 2019; Nakanishi et al., 2016, 2020; Pomares et al., 2012; Sharon et al., 2014; Silva et al., 2013; Sodi et al., 2011; Tian et al., 2017; Zhao et al., 2012). The resulting retinal phenotypes appear to fall into two distinct categories with some overlap. At one extreme is the ARB phenotype with retinal involvement extending from fovea to midperiphery demonstrating intraretinal cystic changes and subretinal serous detachment. The other extreme of biallelic *BEST1* mutations is a VMD-like phenotype normally associated with monoallelic disease demonstrating a vitelliform lesion at the central macula surrounded by near-normal retina. To understand whether there is a genotype-phenotype relationship, we reviewed 139 patients in 25 publications (Birtel et al., 2020; Bitner et al., 2011; Boon et al., 2013; Burgess et al., 2008; Chen et al., 2016; Davidson et al., 2010; Dev Borman et al., 2011; Fung et al., 2015; Habibi et al., 2019; Iannaccone et al., 2011; Jansson et al., 2016; Khan et al., 2018; Kinnick et al., 2011; Kubota et al., 2016; Lee et al., 2015; Luo et al., 2019; Nakanishi et al., 2016, 2020; Pomares et al., 2012; Schatz et al., 2006; Sharon et al., 2014; Silva et al., 2013; Sodi et al., 2011; Tian et al., 2017; Zhao et al., 2012) in terms of their reported genotype and, when possible, we categorized their phenotype based on published OCT data and clinical descriptions. We found 72% (100/139) to have ARB-like phenotype, 12% (17/139) VMD-like phenotype and remaining patients were indeterminate or uncertain. Reported visual acuities were plotted and showed overlap between the phenotypes (Suppl. Fig. S1). In terms of genotype, having both alleles with predicted truncations was more likely to result in ARB phenotype (Birtel et al., 2020; Boon et al., 2013; Burgess et al., 2008; Davidson et al., 2010; Habibi et al., 2019; Pomares et al., 2012) but there were also examples with VMD phenotype (Bitner et al., 2011). Homozygosity for missense mutations Arg255Trp (Luo et al., 2019; Nakanishi et al., 2016, 2020) or Arg141His (Birtel et al., 2020; Boon et al., 2013) caused ARB whereas homozygosity for the missense mutation Arg47Cys (Khan et al., 2018; Kinnick et al., 2011; Sodi et al., 2011) caused VMD phenotype. Frameshift, truncation and splice site mutations could be paired with missense mutations (e.g. Arg255Trp or Ala195Val or Arg141His) to cause ARB phenotype (Birtel et al., 2020; Dev Borman et al., 2011; Kubota et al., 2016; Luo et al., 2019; Nakanishi et al., 2016, 2020; Schatz et al., 2006; Tian et al., 2017), or VMD phenotype (Kinnick et al., 2011). There was even a patient with compound heterozygous missense mutations who appeared to show VMD-like phenotype in one eye and ARB phenotype in the other eye (Zhao et al., 2012). Thus, a clear genotype-phenotype relationship remains elusive. We are aware of the proposed hypothesis that a complete inactivation of *BEST1* gene on both alleles results in ARB phenotype, whereas an allele with a dominant negative effect results in the VMD phenotype (Pomares et al., 2012). However, this hypothesis does not explain the unaffected heterozygous family members of patients with VMD-like phenotype and missense mutations (Kinnick et al., 2011; Lee et al., 2015; Sodi et al., 2011; Tian et al., 2017) or rare ARB phenotype associated with heterozygous missense mutations (Toto et al., 2016). Practically, among all reported patients with biallelic *BEST1* mutations, the more severe ARB phenotype appears to be much more common than the milder VMD phenotype. Our detailed studies herein attempted to provide greater clarity to the ARB phenotype.

Intraretinal and subretinal fluid

RPE cells are key in fluid transport/management as they transport fluid from the photoreceptors to the choroid (Marmor 1990; Strauss 2005). Retinopathies of diverse origins affecting the RPE function can result in serous retinal detachments where fluid accumulates between the photoreceptors and the RPE (Daruich et al., 2015). Both ARB and VMD-like phenotypes of biallelic *BEST1* mutations can show serous retinal detachments which is not surprising considering bestrophin-related disease primarily affects the RPE (Marmorstein et al., 2000). An important distinction between ARB and VMD-like phenotypes, however, is the accumulation of intraretinal fluid only in the former. The combination of intra- and sub-retinal fluid is generally not common and typically observed in patients with chronic central serous retinopathy (Daruich et al., 2015). Specifically, common forms of intraretinal fluid (cystoid macular edema) of inflammatory or ischemic origins do not typically show retinal detachment (Spaide, 2016). Similarly, intraretinal fluid without retinal detachment is often seen in inherited retinal degenerations (Aleman et al., 2008; Hirakawa et al., 1999). It can be hypothesized that ARB phenotype reflects the chronicity of an earlier VMD-like phenotype after vitelliform lesions have been resorbed. However, this hypothesis is refuted by observations of ARB phenotype detectable in very young patients in the first decade of life (Burgess et al., 2008; Dev Borman et al., 2011; Iannaccone et al., 2011). Alternatively, ARB phenotype reflects greater involvement of Muller glial cells in the disease process as compared to the VMD phenotype. Prominence of the ELM detected on imaging patients with ARB phenotype seems to provide some support for this alternative hypothesis.

Rod function deficit

Dysfunction of the rod photoreceptor driven night vision is encountered commonly in a wide range of inherited retinal degenerations. It was generally assumed that loss of function was due to loss of cells (Jacobson et al., 1997, 2000). We now know that a functional deficit can exist in retained photoreceptor cells (Cideciyan et al., 2020; Jacobson et al., 2005; Stunkel et al., 2018). Patients with biallelic *BEST1* mutations and an ARB phenotype showed large retinal regions with substantial loss of dark-adapted rod sensitivity co-localized with retinal structure likely retaining rod nuclei. In addition, there was abnormal slowing of the kinetics of dark-adaptation rate implying a chromophore recycling defect. Correction of BEST1 pathophysiology with gene augmentation (Guziewicz et al., 2018) could improve both rod sensitivity and accelerate the kinetics of rod dark-adaptation. However, it is important to note that there were structural abnormalities at the photoreceptor-RPE interface at the level of cone and rod outer segments. Whether these long-standing abnormalities can be ameliorated by gene therapy remains to be evaluated.

Supplementary Material

Refer to Web version on PubMed Central for supplementary material.

Acknowledgments

Supported by IVERIC Bio, Inc., NEI R01EY06855, Foundation Fighting Blindness, and unrestricted funds from Research to Prevent Blindness.

References

Aleman TS et al. Retinal laminar architecture in human retinitis pigmentosa caused by Rhodopsin gene mutations. Investig. Ophthalmol. Vis. Sci 49, 1580–1591 (2008). [PubMed: 18385078]

Aleman TS et al. RDH12 mutations cause a severe retinal degeneration with relatively spared rod function. Investig. Ophthalmol. Vis. Sci 59, 5225–5236 (2018). [PubMed: 30372751]

Azam M et al. A homozygous p.Glu150Lys mutation in the opsin gene of two Pakistani families with autosomal recessive retinitis pigmentosa. Mol. Vis 15, 2526–2534 (2009). [PubMed: 19960070]

Birtel J et al. Peripapillary sparing in autosomal recessive bestrophinopathy. Ophthalmol. Retin 4, 523–529 (2020).

Bitner H et al. A homozygous frameshift mutation in BEST1 causes the classical form of Best disease in an autosomal recessive mode. Investig. Ophthalmol. Vis. Sci 52, 5332–5338 (2011). [PubMed: 21467170]

Boon CJF et al. Clinical and genetic heterogeneity in multifocal vitelliform dystrophy. Arch. Ophthalmol 125, 1100–1106 (2007). [PubMed: 17698758]

Boon CJF et al. The spectrum of ocular phenotypes caused by mutations in the BEST1 gene. Prog. Retin. Eye Res 28, 187–205 (2009). [PubMed: 19375515]

Boon CJF et al. Autosomal recessive bestrophinopathy: Differential diagnosis and treatment options. Ophthalmology 120, 809–820 (2013). [PubMed: 23290749]

Bowne SJ et al. A dominant mutation in RPE65 identified by whole-exome sequencing causes retinitis pigmentosa with choroidal involvement. Eur. J. Hum. Genet 19, 1074–1081 (2011). [PubMed: 21654732]

Brandl C et al. Mutations in the genes for interphotoreceptor matrix proteoglycans, IMPG1 and IMPG2, in patients with vitelliform macular lesions. Genes (Basel). 8, 170 (2017). [PubMed: 28644393]

Burgess R et al. Biallelic mutation of BEST1 causes a distinct retinopathy in humans. Am. J. Hum. Genet 82, 19–31 (2008). [PubMed: 18179881]

Cehajic-Kapetanovic J et al. Clinical and molecular characterization of PROM1-related retinal degeneration. JAMA Netw. open 2, e195752 (2019). [PubMed: 31199449]

Chen CJ et al. Long-term macular changes in the first proband of autosomal dominant vitreoretinochoroidopathy (ADVIRC) due to a newly identified mutation in BEST1. Ophthalmic Genet. 37, 102–108, 2016. [PubMed: 26849243]

Cideciyan AV & Jacobson SG Leber congenital amaurosis (LCA): Potential for improvement of vision. Investig. Ophthalmol. Vis. Sci 60, 1680–1695 (2019). [PubMed: 31009524]

Cideciyan AV et al. Rod plateaux during dark adaptation in Sorsby's fundus dystrophy and vitamin A deficiency. Investig. Ophthalmol. Vis. Sci 38, 1786–1794 (1997). [PubMed: 9286267]

Cideciyan AV et al. Rod and cone visual cycle consequences of a null mutation in the 11-cis-retinol dehydrogenase gene in man. Vis. Neurosci 17, 667–678 (2000). [PubMed: 11153648]

Cideciyan AV et al. ABCA4-associated retinal degenerations spare structure and function of the human parapapillary retina. Investig. Ophthalmol. Vis. Sci 46, 4739–4746 (2005). [PubMed: 16303974]

Cideciyan AV et al. Reduced-illuminance autofluorescence imaging in ABCA4-associated retinal degenerations. J. Opt. Soc. Am. A 24, 1457 (2007).

Cideciyan AV et al. Human cone visual pigment deletions spare sufficient photoreceptors to warrant gene therapy. Hum. Gene Ther 24, 993–1006 (2013). [PubMed: 24067079]

Cideciyan AV et al. Rod function deficit in retained photoreceptors of patients with class B Rhodopsin mutations. Sci. Rep 10, 12552 (2020). [PubMed: 32724127]

Cideciyan AV et al. Measures of function and structure to determine phenotypic features, natural history, and treatment outcomes in inherited retinal diseases. Annu Rev Vis Sci. 7, 747–772 (2021). [PubMed: 34255540]

Curcio CA, Sloan KR, Kalina RE & Hendrickson AE Human photoreceptor topography. J. Comp. Neurol 292, 497–523 (1990). [PubMed: 2324310]

Daftarian N et al. PRPH2 mutation as the cause of various clinical manifestations in a family affected with inherited retinal dystrophy. Ophthalmic Genet. 40, 436–442 (2019). [PubMed: 31618092]

Daruich A et al. Central serous chorioretinopathy: Recent findings and new physiopathology hypothesis. Prog. Retin. Eye Res 48, 82–118 (2015). [PubMed: 26026923]

Davidson AE et al. A synonymous codon variant in two patients with autosomal recessive bestrophinopathy alters in vitro splicing of BEST1. Mol. Vis 16, 2916–2922 (2010). [PubMed: 21203346]

Dev Borman A et al. Childhood-onset autosomal recessive bestrophinopathy. Arch. Ophthalmol 129, 1088–1093 (2011). [PubMed: 21825197]

Dryja TP et al. A point mutation of the rhodopsin gene in one form of retinitis pigmentosa. Nature 343, 364–366 (1990). [PubMed: 2137202]

Dryja TP, Berson EL, Rao VR & Oprian DD Heterozygous missense mutation in the rhodopsin gene as a cause of congenital stationary night blindness. Nat. Genet 4, 280–283 (1993). [PubMed: 8358437]

Dryja TP, Hahn LB, Reboul T & Arnaud B Missense mutation in the gene encoding the α subunit of rod transducin in the Nougaret form of congenital stationary night blindness. Nat. Genet 13, 358–360 (1996). [PubMed: 8673138]

Farrar GJ et al. A three-base-pair deletion in the peripherin-RDS gene in one form of retinitis pigmentosa. Nature. 354, 478–80 (1991). [PubMed: 1749427]

Freund CL et al. Cone-rod dystrophy due to mutations in a novel photoreceptor-specific homeobox gene (CRX) essential for maintenance of the photoreceptor. Cell. 91, 543–553 (1997). [PubMed: 9390563]

Fuchs S, Nakazawa M, Maw M, Tamai M, Oguchi Y, Gal A. A homozygous 1-base pair deletion in the arrestin gene is a frequent cause of Oguchi disease in Japanese. Nat Genet. 10, 360–2 (1995). [PubMed: 7670478]

Fung AT et al. New BEST1 mutations in autosomal recessive bestrophinopathy. Retina 35, 773–782 (2015). [PubMed: 25545482]

Gerth-Kahlert C et al. Genotype-phenotype analysis of a novel recessive and a recurrent dominant SNRNP200 variant causing retinitis pigmentosa. Investig. Ophthalmol. Vis. Sci 60, 2822–2835 (2019). [PubMed: 31260034]

Guillonneau X et al. A nonsense mutation in a novel gene is associated with retinitis pigmentosa in a family linked to the RP1 locus. Hum Mol Genet. 8, 1541–6 (1999). [PubMed: 10401003]

Guziewicz KE et al. BEST1 gene therapy corrects a diffuse retina-wide microdetachment modulated by light exposure. Proc. Natl. Acad. Sci. U. S. A 115, E2839–E2848 (2018). [PubMed: 29507198]

Habibi I et al. Clinical and genetic findings of autosomal recessive bestrophinopathy (ARB). Genes (Basel). 10, (2019).

Hirakawa H, Iijima H, Gohdo T & Tsukahara S Optical coherence tomography of cystoid macular edema associated with retinitis pigmentosa. Am. J. Ophthalmol 128, 185–191 (1999). [PubMed: 10458174]

Huckfeldt RM et al. Biallelic RP1-associated retinal dystrophies: Expanding the mutational and clinical spectrum. Mol. Vis 26, 423–433 (2020). [PubMed: 32565670]

Hull S et al. The clinical features of retinal disease due to a dominant mutation in RPE65. Mol. Vis 22, 626–635 (2016). [PubMed: 27307694]

Iannaccone A et al. Autosomal recessive Best vitelliform macular dystrophy: Report of a family and management of early-onset neovascular complications. Arch. Ophthalmol 129, 211–217 (2011). [PubMed: 21320969]

Jacobson SG et al. Automated light- and dark-adapted perimetry for evaluating retinitis pigmentosa. Ophthalmology 93, 1604–1611 (1986). [PubMed: 3808619]

Jacobson SG et al. Disease expression in X-linked retinitis pigmentosa caused by a putative null mutation in the RPGR gene. Investig. Ophthalmol. Vis. Sci 38, 1983–1997 (1997). [PubMed: 9331262]

Jacobson SG et al. Retinal degenerations with truncation mutations in the cone-rod homeobox (CRX) gene. Investig. Ophthalmol. Vis. Sci 39, 2417–2426 (1998). [PubMed: 9804150]

Jacobson SG et al. Disease expression of RP1 mutations causing autosomal dominant retinitis pigmentosa. Investig. Ophthalmol. Vis. Sci 41, 1898–1908 (2000). [PubMed: 10845615]

Jacobson SG et al. Identifying photoreceptors in blind eyes caused by RPE65 mutations: Prerequisite for human gene therapy success. Proc. Natl. Acad. Sci. U. S. A 102, 6177–6182 (2005). [PubMed: 15837919]

Jacobson SG et al. Complexity of the class B phenotype in autosomal dominant retinitis pigmentosa due to rhodopsin mutations. Investig. Ophthalmol. Vis. Sci 57, 4847–4858 (2016). [PubMed: 27654411]

Jansson RW et al. Biallelic mutations in the BEST1 gene: Additional families with autosomal recessive bestrophinopathy. Ophthalmic Genet. 37, 183–193 (2016). [PubMed: 26333019]

Jespersgaard C et al. Molecular genetic analysis using targeted NGS analysis of 677 individuals with retinal dystrophy. Sci Rep. 9, 1219 (2019). [PubMed: 30718709]

Johnson AA et al. Bestrophin 1 and retinal disease. Prog. Retin. Eye Res 58, 45–69 (2017). [PubMed: 28153808]

Kajiwara K et al. Mutations in the human retinal degeneration slow gene in autosomal dominant retinitis pigmentosa. Nature. 354, 480–3 (1991). [PubMed: 1684223]

Khan KN et al. Normal electrooculography in Best disease and autosomal recessive bestrophinopathy. Retina 38, 379–386 (2018). [PubMed: 28590961]

Kinnick TR et al. Autosomal recessive vitelliform macular dystrophy in a large cohort of vitelliform macular dystrophy patients. Retina 31, 581–595 (2011). [PubMed: 21273940]

Krämer F et al. Mutations in the VMD2 gene are associated with juvenile-onset vitelliform macular dystrophy (Best disease) and adult vitelliform macular dystrophy but not age-related macular degeneration. Eur. J. Hum. Genet 8, 286–292 (2000). [PubMed: 10854112]

Kubota D et al. Detailed analysis of family with autosomal recessive bestrophinopathy associated with new BEST1 mutation. Doc. Ophthalmol 132, 233–243 (2016). [PubMed: 27071392]

Lamb TD & Pugh EN Dark adaptation and the retinoid cycle of vision. Prog. Retin. Eye Res 23, 307–380 (2004). [PubMed: 15177205]

Lee CS et al. A novel BEST1 mutation in autosomal recessive bestrophinopathy. Investig. Ophthalmol. Vis. Sci 56, 8141–8150 (2015). [PubMed: 26720466]

Lee W et al. The external limiting membrane in early–onset Stargardt disease. Investig. Ophthalmol. Vis. Sci 55, 6139–6149 (2014). [PubMed: 25139735]

Luo J et al. Novel BEST1 mutations and special clinical characteristics of autosomal recessive bestrophinopathy in Chinese patients. Acta Ophthalmol. 97, 247–259 (2019). [PubMed: 30593719]

Marlhens F et al. Mutations in RPE65 cause Leber's congenital amaurosis. Nat. Genet 17, 139–141 (1997). [PubMed: 9326927]

Marmor MF Control of subretinal fluid: Experimental and clinical studies. Eye 4, 340–344 (1990). [PubMed: 2199242]

Marmorstein AD et al. Bestrophin, the product of the best vitelliform macular dystrophy gene (VMD2), localizes to the basolateral plasma membrane of the retinal pigment epithelium. Proc. Natl. Acad. Sci. U. S. A 97:12758–12763 (2000). [PubMed: 11050159]

Marmorstein AD, Cross HE & Peachey NS Functional roles of bestrophins in ocular epithelia. Prog. Retin. Eye Res 28, 206–226 (2009). [PubMed: 19398034]

Marmorstein AD et al. Mutant Best1 expression and impaired phagocytosis in an iPSC model of autosomal recessive bestrophinopathy. Sci Rep. 8, 4487 (2018). [PubMed: 29540715]

Marquardt A et al. Mutations in a novel gene, VMD2, encoding a protein of unknown properties cause juvenile-onset vitelliform macular dystrophy (Best's disease). Hum. Mol. Genet 7, 1517–1525 (1998). [PubMed: 9700209]

Maruko I, Iida T, Spaide RF & Kishi S Indocyanine green angiography abnormality of the periphery in vitelliform macular dystrophy. Am. J. Ophthalmol 141, 976–978 (2006). [PubMed: 16678528]

Maw MA et al. A frameshift mutation in prominin (mouse)-like 1 causes human retinal degeneration. Hum Mol Genet. 9, 27–34 (2000). [PubMed: 10587575]

Miller SA Multifocal Best's vitelliform dystrophy. Arch. Ophthalmol 95, 984–990 (1977). [PubMed: 869757]

Naeem MA et al. GNAT1 associated with autosomal recessive congenital stationary night blindness. Invest Ophthalmol Vis Sci. 53, 1353–1361 (2012). [PubMed: 22190596]

Nakanishi A et al. Clinical and genetic findings of autosomal recessive bestrophinopathy in Japanese cohort. Am. J. Ophthalmol 168, 86–94 (2016). [PubMed: 27163236]

Nakanishi A et al. Changes of cone photoreceptor mosaic in autosomal recessive bestrophinopathy. Retina 40, 181–186 (2020). [PubMed: 30308565]

Palczewski K & Kiser PD Shedding new light on the generation of the visual chromophore. Proc. Natl. Acad. Sci. U. S. A 117, 19629–19638 (2020). [PubMed: 32759209]

Perrault I et al. Retinal dehydrogenase 12 (RDH12) mutations in Leber congenital amaurosis. Am. J. Hum. Genet 75, 639–646 (2004). [PubMed: 15322982]

Petrukhin K et al. Identification of the gene responsible for best macular dystrophy. Nat. Genet 19, 241–247 (1998). [PubMed: 9662395]

Pomares E et al. Nonsense-mediated decay as the molecular cause for autosomal recessive bestrophinopathy in two unrelated families. Investig. Ophthalmol. Vis. Sci 53, 532–537 (2012). [PubMed: 22199244]

Richards S et al. Standards and guidelines for the interpretation of sequence variants: a joint consensus recommendation of the American College of Medical Genetics and Genomics and the Association for Molecular Pathology. Genet Med. 17, 405–24 (2015). [PubMed: 25741868]

Rosenfeld PJ et al. A null mutation in the rhodopsin gene causes rod photoreceptor dysfunction and autosomal recessive retinitis pigmentosa. Nat. Genet 1, 209–213 (1992). [PubMed: 1303237]

Sarkar H, Dubis AM, Downes S & Moosajee M Novel heterozygous deletion in retinol dehydrogenase 12 (RDH12) causes familial autosomal dominant retinitis pigmentosa. Front. Genet 11, 335 (2020). [PubMed: 32322264]

Schatz P, Klar J, Andréasson S, Ponjavic V & Dahl N Variant phenotype of Best vitelliform macular dystrophy associated with compound heterozygous mutations in VMD2. Ophthalmic Genet. 27, 51–56 (2006). [PubMed: 16754206]

Seddon JM et al. Assessment of mutations in the Best macular dystrophy (VMD2) gene in patients with adult-onset foveomacular vitelliform dystrophy, age-related maculopathy, and bull's-eye maculopathy. Ophthalmology 108, 2060–2067 (2001). [PubMed: 11713080]

Sharon D et al. Ocular phenotype analysis of a family with biallelic mutations in the BEST1 gene. Am. J. Ophthalmol 157, 697–709.e1–2. (2014). [PubMed: 24345323]

Sharon D, Wimberg H, Kinarty Y & Koch KW Genotype-functional-phenotype correlations in photoreceptor guanylate cyclase (GC-E) encoded by GUCY2D. Prog. Retin. Eye Res 63, 69–91 (2018). [PubMed: 29061346]

Silva RA, Berrocal AM, Lam BL & Albini TA Novel mutation in BEST1 associated with retinoschisis. JAMA Ophthalmol. 131, 794–798 (2013). [PubMed: 23572118]

Sodi A et al. A novel mutation in the VMD2 gene in an Italian family with Best maculopathy. J. Fr. Ophtalmol 30, 616–620 (2007). [PubMed: 17646752]

Sodi A et al. Ocular phenotypes associated with biallelic mutations in BEST1 in Italian patients. Mol. Vis 17, 3078–3087 (2011). [PubMed: 22162627]

Spaide RF Retinal vascular cystoid macular edema: Review and new theory. Retina 36, 1823–1842 (2016). [PubMed: 27328171]

Strauss O The retinal pigment epithelium in visual function. Physiol. Rev 85, 845–881 (2005). [PubMed: 15987797]

Stunkel ML et al. Expanded retinal disease spectrum associated with autosomal recessive mutations in GUCY2D. Am. J. Ophthalmol 190, 58–68 (2018). [PubMed: 29559409]

Sullivan LS et al. A novel dominant mutation in SAG, the Arrestin-1 gene, is a common cause of retinitis pigmentosa in Hispanic families in the southwestern United States. Invest Ophthalmol Vis Sci. 58, 2774–2784, (2017). [PubMed: 28549094]

Tian L et al. Screening of BEST1 gene in a Chinese cohort with Best vitelliform macular dystrophy or autosomal recessive bestrophinopathy. Investig. Ophthalmol. Vis. Sci 58, 3366–3375 (2017). [PubMed: 28687848]

Toto L et al. Bestrophinopathy: A spectrum of ocular abnormalities caused by the c.614T>C mutation in the BEST1 gene. Retina 36, 1586–1595 (2016). [PubMed: 26716959]

Wang X et al. Comprehensive molecular diagnosis of 179 Leber congenital amaurosis and juvenile retinitis pigmentosa patients by targeted next generation sequencing. J Med Genet. 50, 674–88 (2013). [PubMed: 23847139]

Yardley J et al. Mutations of VMD2 splicing regulators cause nanophthalmos and autosomal dominant vitreoretinochoroidopathy (ADVIRC). Investig. Ophthalmol. Vis. Sci 45, 3683–3689 (2004). [PubMed: 15452077]

Zhao L et al. A novel compound heterozygous mutation in the BEST1 gene causes autosomal recessive Best vitelliform macular dystrophy. Eye 26, 866–871 (2012). [PubMed: 22422030]

Highlights

- Detailed multimodal phenotype in patients with autosomal recessive bestrophinopathy
- Prominence of external limiting membrane pointing to activation of glial cells
- Perimacular regions with retained rod photoreceptors lack co-localized rod function
- The kinetics of rod dark-adaptation is abnormally slow
- Night vision-based outcome measures could show improvement with successful therapy

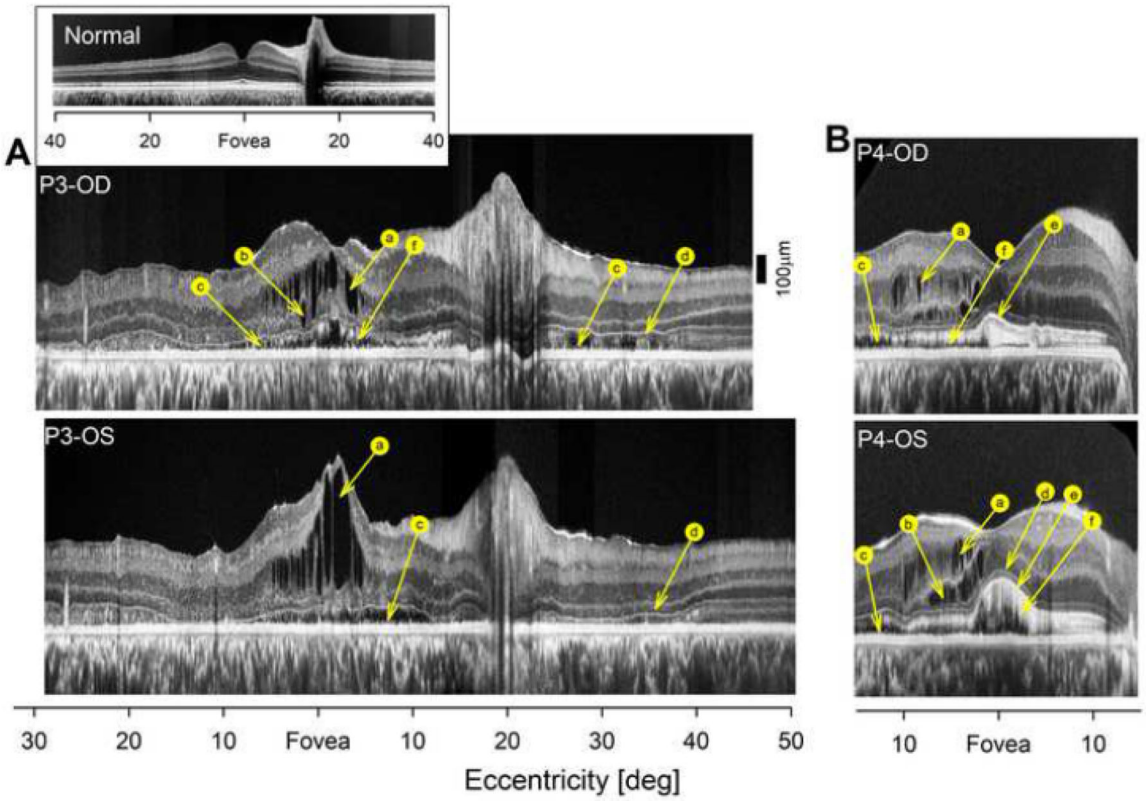

Figure 1:

Ultra-high resolution OCTs in both eyes of P3 and P4 compared to a representative normal eye. Scans are along the horizontal meridian crossing the fovea. All scans are shown as equivalent right eyes for comparability. Features labeled are: a, intraretinal fluid in the inner nuclear layer; b, intraretinal fluid in the outer nuclear layer; c, subretinal fluid; d, enhanced reflection originating from the external limiting membrane; e, locally enhanced reflection originating from near the junction between inner and outer segments; f, stalactite-like reflective material extending into subretinal space. For both eyes of P3, ultra-wide angle OCTs are generated by digital stitching.

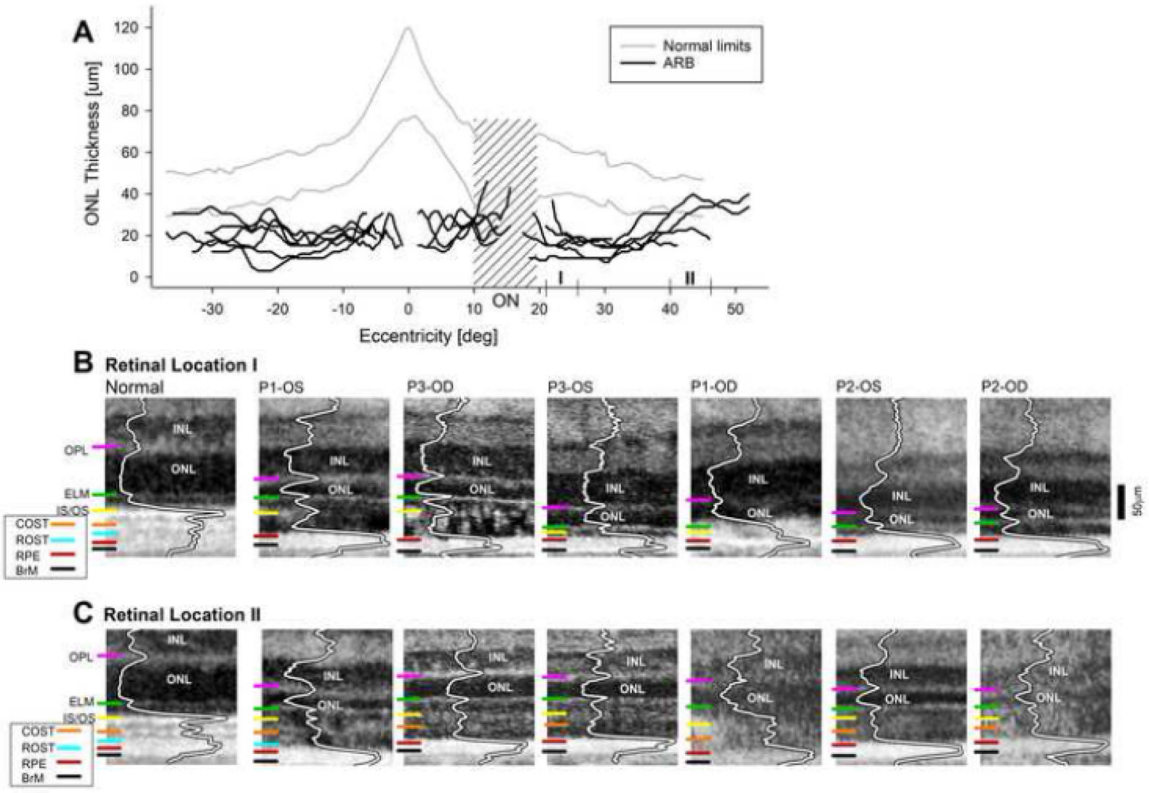

Figure 2:

Outer retinal structure in patients with biallelic *BEST1* mutations. (**A**) ONL thickness in six *BEST1* eyes (thicker black traces) as compared to normal limits (gray traces). I and II in the nasal retina (Nr) demarcate retinal locations further analyzed in detail in panels B and C. ON=optic nerve head (hashed). (**B,C**) Identifiable outer retinal peaks in six *BEST1* eyes compared to normal at retinal locations I (B) and II (C). White traces show the longitudinal reflectivity profiles. INL=inner nuclear layer, ONL=outer nuclear layer, OPL=outer plexiform layer, ELM=external limiting membrane, IS/OS=junction between inner and outer segments, COST=cone outer segment tips, ROST=rod outer segment tips, RPE=retinal pigment epithelium, BrM=Bruch's membrane.

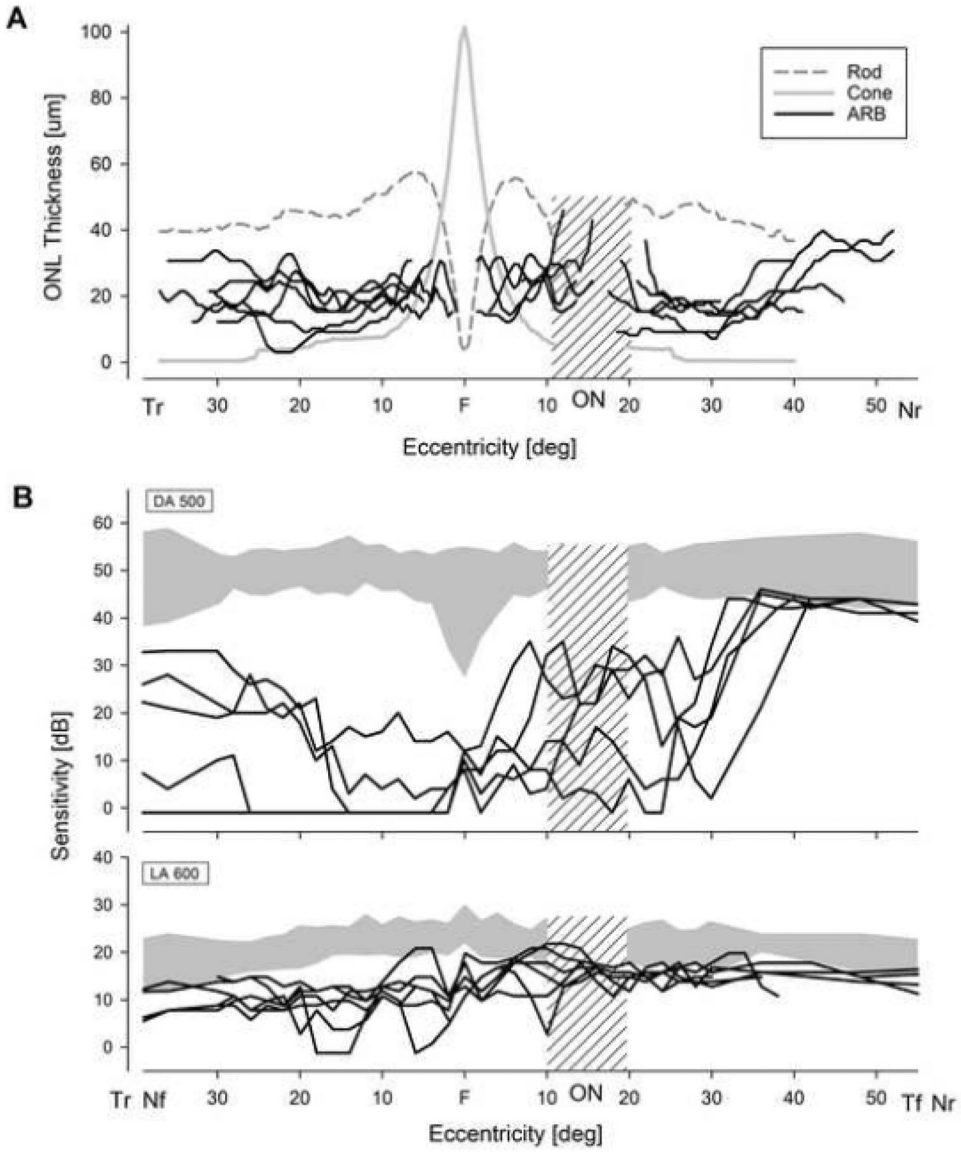

Figure 3:

Colocalization of ONL thickness and rod and cone function. (**A**) ONL thickness in six *BEST1* eyes (thicker black traces, duplicated from Fig.2) as compared to estimated normal cone (gray) or rod (dashed) ONL thickness. Only retinal locations without detectable cystic changes in the ONL layer have been quantified. At eccentricities beyond the parafovea, *BEST1* eyes retain ONL thickness greater than expected from a cone-only ONL and thus likely contain surviving rod photoreceptors. Tr, temporal retina; Nr, nasal retina. (**B**) Dark-adapted 500 nm (DA 500, upper panel) and light-adapted 600 nm (LA 600, lower panel) sensitivities co-localized with the ONL thickness measurements shown in (A). Gray bands depict normal limits. Large losses of rod sensitivity with DA 500 are inconsistent with retained rod photoreceptors and imply a treatment potential. Nf, nasal visual field; Tf, temporal visual field. Expected location of the optic nerve is shown by hashing.

Table 1:

Demographics and genetics of *BEST1*-ARB patients

							VA (logMAR)		Refraction	
Patient	**Sex**	**Allele1**[a]		**Allele2**[a]		**Age**	**RE**	**LE**	**RE**	**LE**
P1	F	c.341T>C	p.(Val114Ala)	c.400C>G	p.(Leu134Val)	39	0.58	0.72	−0.75−0.75 × 99[c]	+0.50 − 1.00 × 6[c]
P2[b]	M	c.95T>C	p.(Leu32Pro)	c.102C>T	p.(Gly34Gly)	36	0.54	0.36	+2.50 − 0.25 × 46	+0.25 − 0.75 × 80
P3[b]	M	c.95T>C	p.(Leu32Pro)	c.102C>T	p.(Gly34Gly)	31	0.48	0.70	−1.25−0.25 × 120	plano
P4	F	c.763C>T	p.(Arg255Trp)	c.948+1delG	-	22	0.08	0.18	−1.00DS	plano − 1.50 × 10

[a] NM_004183.4

[b] siblings

[c] IOL